Chapter One

Introduction to Quantum Cascade Lasers

1.1 Introduction

In 1994, the quantum cascade laser emerged as an innovative and unique semiconductor device operating in the infrared (IR) region of the spectrum. Since that time the QCL has inspired a large body of scientific research, and today occupies a key position within the field of IR spectroscopy, where it provides the basis for many modern spectroscopic systems. As will be shown over the course of this thesis, QCLs differ radically from conventional semiconductor lasers, both in the way they generate light, and in the range of wavelengths at which different devices can operate. QCLs are *unipolar* devices; i.e. only electrons are involved in the process of generating photons, which are produced when electrons make *intersubband* optical transitions between confined energy states within the conduction band of the QCL structure. This is in direct contrast to devices such as, for example, semiconductor diode lasers which produce light through the recombination of electrons and holes across an energy bandgap. The design scheme of the QCL is extremely flexible, and allows a large variation in output wavelength through judicious tailoring of the energy levels involved in the optical transition - optical output is not necessarily limited by the material from which a device is fabricated. This wavelength flexibility, combined with the fact that many molecules have rotational and vibrational modes resonant with energies corresponding to the mid-infrared portion of the spectrum, means that QCLs now fulfil a vital role at the heart of many gas sensing applications[1,2]. Gases such as methane (CH_4), ammonia (NH_3), sulphur dioxide (SO_2) and carbon monoxide (CO) to name but a few all have absorption peaks in the mid-infrared, and can thus be detected by spectroscopic systems that incorporate a QCL with the appropriate operating wavelength. Gas sensing applications

that utilise mid-infrared lasers also benefit from two atmospheric windows that exist at approximately $3 \leq \lambda \leq 5\mu m$ and $8 \leq \lambda \leq 14\mu m$, in which the attenuation of IR radiation by water vapour in the atmosphere is at a minimum. QCL-based technologies have now been successfully commercialised into products that offer detection at the parts per million to parts per billion level for a diverse range of gases in various settings. These include waste and pollutant monitoring in industrial installations as well as the natural environment[3-5]. Other areas of exploitation include QCL laser systems for so-called infrared countermeasures - applications that involve confusing the radar and guidance systems typically found in military hardware[6] - counter-terrorism applications in the form of explosive detection[7] and breath analysis for health monitoring[8].

1.2 Thesis Outline

This thesis presents an experimental study of gallium-arsenide (GaAs) based quantum cascade lasers (QCLs), with an emphasis on enhancing device performance through optimisation of the laser waveguide structure. Chapter one gives a general introduction to the quantum cascade laser, firstly from an historical perspective, before then introducing the basic concepts behind QCL design and operation. Chapter two discusses some of the theoretical tools that can be used to qualitatively predict key QCL parameters, while chapter three outlines the processes involved in the fabrication and characterisation of the devices presented in the subsequent experimental sections of this thesis. Chapter four begins with a discussion of QCL waveguides as they relate to GaAs-based devices, which is followed by a detailed presentation of the design and performance of GaAs/AlGaAs QCLs which incorporate indium-gallium-phosphide (InGaP) and indium-aluminium-phosphide (InAlP) layers to form the device waveguide. A comparison of their performance relative to previous GaAs-based lasers is also given. Chapter five concerns the optimisation of QCLs with InAlP waveguides, particularly with regard to the large operating voltages that are a feature of the devices presented in chapter four. Again, several different device designs are described and their corresponding operating characteristics compared. Chapter six describes several QCLs with InGaP waveguides, high-reflectivity facet coatings and a redesigned active region that have been observed to operate in continuous-wave mode - an important

advancement in device efficiency when compared to the previous lasers operating in pulsed mode. Finally, chapter seven provides a summary of all experimental work carried out, conclusions that may be drawn from the results and a discussion of the likely direction of future studies.

1.3 Historical Development of the Quantum Cascade Laser

The quantum cascade laser has a development history stretching back over forty years, beginning with the pioneering work of two Soviet physicists who laid the theoretical foundations upon which subsequent applied developments would build. In 1971, Kazarinov and Suris[9] first suggested the possibility that electromagnetic waves might be amplified by a semiconductor superlattice under the influence of an external electric field, due to the optical transitions of electrons between confined states within the lattice quantum wells. Due to limitations in the semiconductor growth techniques of the time, it was not possible to produce the extremely thin and abrupt semiconductor layers required to form these superlattices, and over a decade would pass before the ideas proposed by Kasarinov and Suris could be applied and developed in the laboratory. By the mid-1980s however, semiconductor growth technology had advanced sufficiently to allow the fabrication of high quality semiconductor superlattices, and soon after, the first investigations into the nature of the intersubband transitions within these structures were being carried out.

Intersubband absorption in a semiconductor quantum well was first observed by West and Eglash[10] in 1985, who used an infrared laser incident on a 50-period GaAs/AlGaAs superlattice to probe the absorption due to the quantised conduction band states corresponding to energies of 152meV and 121meV (8.2μm and 10.2μm). Observation of intersubband emission followed soon after, when Helm and co-workers reported infrared emission from three conduction band energy levels of a GaAs/AlGaAs superlattice at 50μm, 69μm and 113μm[11]. Sandwiched between these two important observations was the first report, by Capasso et al, of resonant tunnelling of electrons through an InGaAs/AlInAs semiconductor superlattice[12]. With the superlattice placed

under an appropriate electric field, several peaks in photocurrent were observed corresponding to the alignment of the confined quantum well ground state with an excited state of the adjacent well. Under these conditions, electrons can resonantly tunnel between the wells from ground to excited state through the intervening AlInAs barriers. Electrons can then transition (non-radiatively in this case) to the ground state before tunnelling into the next well. This process of resonant electron tunnelling, whereby electrons 'cascade' through a superlattice structure, is key to the operation of the QCL.

In parallel with these experimental breakthroughs, theoretical work was being published that forwarded various proposals for infrared lasers that would utilise the very same intersubband transitions and resonant tunnelling processes. In 1986 Yuh and Wang[13] proposed an intersubband laser consisting of a semiconductor superlattice divided into three distinct sections; an active region in which electrons would make optical transitions between an upper and lower miniband of electronic states within the conduction band, and two regions either side of this from which electrons would be injected into, and extracted from the active region via appropriately aligned minibands. Population inversion would be maintained via the current injected into the upper miniband of the injection region, while the wavelength of the device would be tailored by altering the energy spacing of the upper and lower active region minibands. A second proposal, presented by Liu[14], suggested a GaAs/AlGaAs superlattice in which optical transitions would be made by electrons transitioning between the confined states within the quantum wells, rather than the minibands proposed by Yuh and Wang. As had been experimentally demonstrated by Capasso et al, once a transition had been made between the upper level and the ground state - and provided the states were suitably aligned - electrons could resonantly tunnel between wells into the next excited state before making another optical transition. This process would be repeated along the entire superlattice structure, with the requisite population inversion being achieved by ensuring that the tunnelling time through the barriers was shorter than the lifetime of the radiative transitions within the quantum wells.

Much of this experimental and theoretical work would be brought together when, in 1994, Faist et al[15] reported the first demonstration of working laser based on intersubband transitions within the conduction band of a semiconductor superlattice. This device - christened the quantum cascade laser - would kick-start a new field of

infrared laser physics and lead to a burgeoning interest in such devices. The laser itself was based on the InGaAs/AlInAs/InP material system, with a core comprising of 25 repeated periods of a 3-quantum well active region followed by a superlattice of wells and barriers forming an injection region. The core was surrounded by a waveguide formed by an upper layer of AlInAs, while the InP substrate acted as the lower portion of the waveguide. A perceived stumbling block to the experimental realisation of the QCL had been the notion that laser action would be severely compromised by the rate of non-radiative optical phonon scattering of electrons - which occurs on a picosecond scale - being much faster than the nanosecond-scale rate of radiative spontaneous emission. It was assumed that this would make device operation prohibitively inefficient, and also limit any emission that may be possible to energies below that of the LO phonon energy (~34meV for InGaAs), i.e. the far infrared. Faist and co-workers however, were the first to realise that once lasing had been achieved, the rate of *stimulated* photon emission would approach that of the non-radiative LO phonon scattering, thereby greatly increasing the efficiency of the device active region[16]. Their new laser generated photons via the optical electronic transitions between a confined upper and lower state within the active region quantum wells, which had an energy separation such that emission was observed at λ=4.2μm. Electrons would then transition from the lower state to a closely spaced ground-state via non-radiative LO phonon-assisted scattering, before resonantly tunnelling into an adjacent injector region. Population inversion within the active region was enhanced by tailoring the energy spacing of the lower and ground state to be similar to that of the LO phonon energy, ensuring the rate at which the lower electronic states were depopulated was significantly faster than the non-radiative scattering between the two laser levels - ~0.5ps compared to ~4.3ps. The QCL was operational up to a temperature of 88K, with output power approaching 10mW at 10K.

While the performance levels of this groundbreaking device were low by the standards of modern QCLs, the Faist group soon made rapid inroads in the quest for improved performance levels. Only twelve months would pass before continuous wave operation was reported[17], with room-temperature pulsed operation following shortly after[18,19]. Lower device threshold currents and higher output powers were an inevitable consequence of this research drive, as was the milestone that was the realisation of a QCL capable of CW operation at room temperature in 2001[20]. The large interest in

QCLs that this pioneering work inspired means that QCLs can now be designed to operate at a wide range of wavelengths varying from ~3μm at the short-end of the mid-IR[21], up to the far-infrared THz regime[22]. Devices operating in the range $4\mu m \lesssim \lambda \lesssim 5\mu m$ in the mid-IR now routinely achieve room-temperature CW operation at output powers greater than 1W[23-25], while spectroscopic applications are well provided for by lasers that have a broad gain spectrum (in some cases up to $400cm^{-1}$), and whose output can be tuned over a large wavelength range using an external cavity system[26]. Other areas in which QCLs now find an application include non-linear optics[27,28], in which effects such as second harmonic generation can be utilised to further enhance the wavelength range offered by devices.

1.4 Basic Principles of the Quantum Cascade Laser

The core region of a QCL consists of multiple quauntum wells and barriers formed from two semiconductor materials with a differing bandgap - the material with the smaller bandgap constituting the well, and the larger gap material forming the barriers either side. The height of the quantum well is determined by the way in which the two bands align themselves - i.e. the conduction band offset - and varies between material systems, being around 390meV for GaAs/AlGaAs and 520meV for InGaAs/AlInAs[29]. Shown in figure 1.1 is part of the biased conduction band offset for the core region of a GaAs/AlGaAs QCL, encompassing an active region followed by an injection region - which together constitute one core region period - followed by a second active region. A complete QCL core region can be comprised of up to around fifty repeats of these periods.

The active region on the left of the figure is made up of three quantum wells (although active regions featuring four wells are also common), and the moduli squared of the first three confined electronic states associated with these wells at energy levels E_3, E_2 and E_1 are shown in red. Assuming an electron is injected into the upper state E_3 from the preceding injector region, an optical transition can take place between $E_3 \rightarrow E_2$ resulting in the emission of a photon (represented by the green arrow), where the emission wavelength is determined by the energy separation of E_3 and E_2. The electron then quickly scatters to the lower state E_1 where it can tunnel into the injector region. The

states within the injector form a miniband (encompassed by the hatched area in figure 1.1) allowing the electron to traverse this region before tunnelling through the injection barrier and into the upper state E_3 of the next active region, via the injector state E_i. It can be seen that there are no injector region states resonant with the upper level E_3 in the direction of electron travel, and this so-called minigap reduces the probability of the non-radiative escape of electrons from this level. The process of optical transition, followed by injection into the next active region is then repeated over the length of the device core region. In this way, it is possible for a single electron to emit photons at each active region, and thus QCLs tend to have a large optical gain in comparison to conventional semiconductor lasers. This 'recycling' of electrons also leads to large optical output powers - often measured in Watts[30] - as output power is proportional to the number of core region periods within a device.

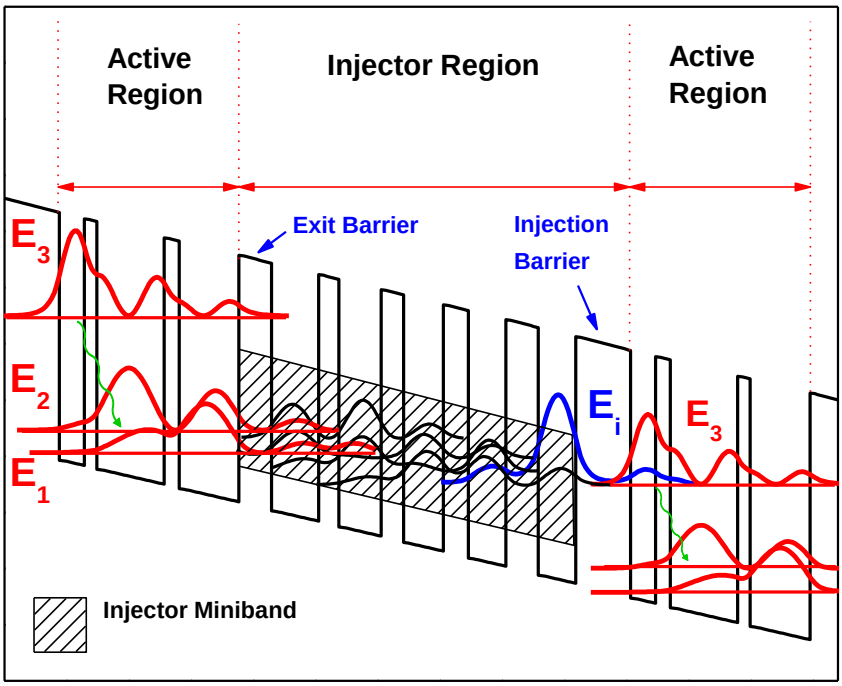

Figure 1.1: Schematic diagram showing a QCL core divided into its constituent active and injection regions. The optical transition between upper and lower laser levels ($E_3 \rightarrow E_2$ in red) is denoted by the green wavy arrow.

Population inversion between the upper and lower states is achieved by ensuring that the electron lifetime in the upper state E_3 is greater than that of the lower states E_2 and E_1. A detailed analysis of QCL scattering times and population inversion is presented in chapter two.

The device emission wavelength can be controlled by adjusting the position of the electronic states within the active region, primarily through variation in the width of the quantum wells and barriers. This is in direct contrast to interband lasers in which the wavelength is determined by the band gap - a property of the material system itself - and means that for a QCL, a wide range of wavelengths can be achieved for a particular material. GaAs QCLs for example, have exhibited emission over wavelengths spanning λ~7μm on the shorter side[31], up to λ>100μm in the case of modern THz devices[22].

1.5 Active Region Design

Three and four-well active regions

The large scope for variation in the sequence of quantum wells and barriers that constitute the core region of a QCL structure has led to a range of differing active region designs. Through systematic adjustment to the number and width of the active region wells and barriers, parameters such as emission wavelength, injection efficiency and electron scattering rates can all be controlled. One of the most common active region configurations currently utilised consists of either three or four quantum wells[32,33], bounded by an injection and exit barrier through which electrons enter and exit the active region respectively (see figure 1.1). As demonstrated by Faist et al, the population inversion attainable between the upper and lower laser levels can be dramatically increased by ensuring the energy spacing between the two (or more) lower levels is approximately equal to that of an LO phonon in the well material - $\hbar\omega_{LO}$~36meV for GaAs - which allows the electron scattering lifetime between these levels to be significantly reduced through resonance with LO phonon emission. Lifetimes of the order of 0.4ps in the case of three-well designs, and 0.25ps for four-well active regions have been demonstrated, in comparison to over 1ps for electron scattering from the upper laser level to lower levels. These short lower level lifetimes aid rapid depopulation of the lower laser level and increase both the overall population inversion within the active region, and the optical gain required for lasing.

A further benefit of the three and four-well active regions is the control they allow over the coupling between the upper laser level and the injector level, which can be enhanced through adjustment to the width of the thin quantum well adjacent to the injection

barrier. This allows electrons to be injected into the active region with increased efficiency, and reduces the probability of direct non-radiative transitions from the injector region to the lower laser levels. As well as controlling electron lifetimes at particular energy levels within the active region, the spatial nature of the optical transition itself can also be engineered. As will be expanded upon in chapter two, the active region can be tailored such that upper state electron wavefunction primarily occupies either the first or second active region quantum well. In the case of the former, transitions will occur between wells and across the well-barrier interface in a so-called diagonal transition, whereas in the latter the transition will be vertical, taking place between confined states within the same quantum well. Whether optical transitions are diagonal or vertical has consequences for the transition probability, upper laser level lifetime and ultimately the population inversion within the active region.

Bound-to-continuum and continuum-to-continuum active regions:

The bound-to-continuum (BTC) active region design[34], shown in figure 1.2, aims to reproduce the good injection efficiency associated with three and four-well active regions, whilst increasing the efficiency with which electrons are typically extracted from the lower laser levels into the injector. In the case of the four-well design, the rate at which electrons resonantly tunnel through the exit barrier from the lowest laser levels into the injector region is around 10 times slower than the rate of electron scattering between the lower levels themselves (1ps compared to 0.1ps respectively). This discrepancy can lead to a reduction in population inversion through the build-up of electrons in the lower levels[29], particularly at higher temperatures where electrons are able to repopulate these levels through thermal backfilling. The BTC active region addresses this issue by replacing the discrete lower levels with a continuum of electronic states similar to that found within the injector of standard QCL active region designs.

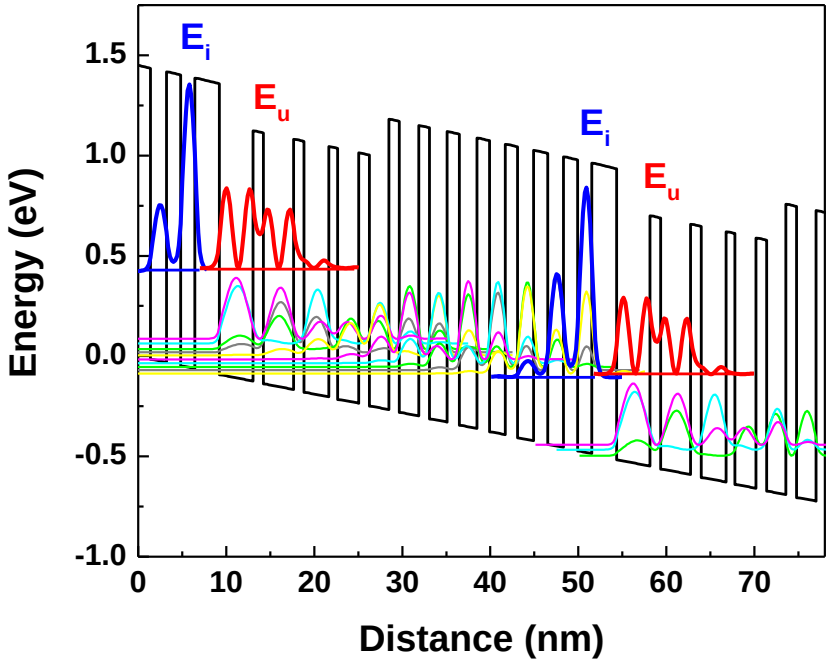

Figure 1.2: QCL Γ-point conduction band profile illustrating the bound-to-continuum active region concept. Optical transitions take place between the upper laser level E_u (shown in red) and a lower continuum of electronic states (multicoloured), before electrons relax along the injector region and are re-injected into the next active region via the state E_i (blue).

This arrangement is achieved by incorporating into the core region a superlattice structure comprising of a series of quantum wells that decrease in width in the direction of electron travel. Rather than the discrete active and injector regions that comprise the core of QCLs featuring three and four-well designs, this structure results in a core with less differentiation between active and injector regions, and a configuration of electronic states in which optical transitions occur between a single discrete upper state, and a lower continuum of states. The advantage of this continuum lies in the fact that electrons scatter through the lower states on a sub-picosecond timescale, avoiding the potential build-up of electrons that can occur in the lower laser levels of the three and four-well designs. Injection efficiency is maintained since electrons continue to be injected from the miniband into the next upper laser level via resonant tunnelling, as is the case with three and four-well active regions.

A further consequence of the BTC design is the broad gain spectrum that arises from the optical transitions between the upper laser level and the large number of states within the lower miniband. This is beneficial for spectroscopic application in which a degree of

wavelength tuning of the laser output is required, for example when analysing gases containing multiple molecule types which would be expected to have several absorption lines at different wavelengths. The gain spectrum can be further widened by extending the concept of the bound to continuum active region to a continuum to continuum design, in which optical transitions are made between an upper and lower continuum, rather than the discrete upper level as for the BTC design. The increase in the number and energy range of states from which optical transitions take place can result in a suitably broadened gain spectrum, with widths of up to 430cm^{-1} being recently reported[35].

1.6 Material Systems for QCL Fabrication: Benefits and Disadvantages of GaAs

To-date, QCL research has primarily focussed on two particular III-V semiconductor compounds as a basis for the fabrication of device structures; namely indium-phosphide (InP) and gallium-arsenide (GaAs). Historically, InP-based devices have attracted a far greater proportion of research, due mainly to the superior device performance that can be achieved when compared to QCLs based on the GaAs material system. It was a QCL featuring an InGaAs/AlInAs active region, grown lattice matched to an InP substrate that first demonstrated lasing in 1994, and since that time the range of materials from which InP-based QCLs have been fabricated has increased to include systems such as InGaAs/AlAsSb[36] and InGaAs/AlAs[37,38]. The first devices developed using the GaAs material system appeared in 1998[39], four years after the emergence of the first InP-based QCLs. Although Page and co-workers reported achievements such as room temperature pulsed operation[40], and low-temperature (150K) continuous wave operation[41] a relatively short time after this, subsequent progress has become somewhat sporadic, with the result being that the CW performance reported by Page et al over a decade ago has yet to be surpassed. The reasons for the lack of progress in relation to GaAs devices can mainly be attributed to its intrinsic material properties, and the kind of performance levels that these properties afford QCLs. For example, the shallow conduction band offset of ΔE_c=0.39eV afforded by GaAs/AlGaAs active regions limits device emission wavelengths to $\lambda \approx 8\mu m$ and above, while also increasing the probability of electron

escape from the upper laser level into the continuum states that exist above the top of the conduction band. This non-radiative escape channel can act to reduce the population inversion between upper and lower laser levels and thus restrict device performance. Also, since the LO phonon-mediated electron scattering lifetime within the QCL active region is essentially inversely proportional to the electron effective mass (m^*)[42], the comparatively large $m^*=0.067m_0$ possessed by GaAs leads to reduced scattering lifetimes in comparison to InP-based devices ($m^*=0.043m_0$ for InGaAs), and thus lower levels of population inversion and gain. A detailed description of the physics of QCL active regions, including a comprehensive analysis of electron lifetimes, scattering rates and population inversion is presented in chapter two.

This seeming inferiority inherent in the material characteristics of GaAs does not necessarily preclude it as a viable QCL material however, and indeed there are certain advantages to utilising this material system over the more commonly used InP. GaAs is one of the most widely studied of all the III-V semiconductor compounds and its production has been successfully implemented on the industrial scale. This has obvious economical benefits for any attempt to mass-produce GaAs-based devices. The fact that $Al_xGa_{1-x}As$ is lattice matched to GaAs for all values of x allows for flexibility in active region design without the need for strain compensation, while also easing the growth constraints for the GaAs/AlGaAs active regions since only the Al source needs to be switched during growth. Nevertheless, the material properties of GaAs can still be regarded as something of a drawback when compared to InP and its associated material systems. One strategy for overcoming these limitations is to focus less on fundamental material properties and more on areas of overall device design in an effort to improve performance. In this respect, a promising area of investigation involves improvements to the QCL waveguide used to confine the optical mode within the device active region. In the case of GaAs-based devices, the waveguide is usually formed using either highly-doped GaAs or high aluminium content $Al_{0.9}Ga_{0.1}As$, both of which have drawbacks associated with their use. In the case of highly-doped GaAs, optical losses can be very high due to free-carrier absorption, while $Al_{0.9}Ga_{0.1}As$ can exhibit poor electrical characteristics. A detailed discussion of the disadvantages of conventional GaAs QCL waveguides is presented in chapter four, while the use of alternative semiconductor materials as QCL waveguides - in an attempt to overcome the limitations of GaAs and AlGaAs, and improve device performance - will form a major part of this thesis.

1. A. A. Kosterev and F. K. Tittel, *Chemical sensors based on quantum cascade lasers*, IEEE Journal of Quantum Electronics, **38**, 582-591, (2002).

2. A. Kosterev, G. Wysocki, Y. Bakhirkin, S. So, R. Lewicki, M. Fraser, F. Tittel and R. F. Curl, *Application of quantum cascade lasers to trace gas analysis*, Applied Physics B-Lasers and Optics, **90**, 165-176, (2008).

3. *Pranalytica [Online]*, Available at: http://www.pranalytica.com/index.php, (2013).

4. *Quantum cascade lasers, mid infrared spectroscopy gas analysers from Cascade Technolgies [Online]*, Available at: http://www.cascade-technologies.com, (2013).

5. *QuantaRed Technologies - Oil in Water Analyzers [Online]*, Available at: http://quantared.com, (2013).

6. R. Maulini, A. Lyakh, A. G. Tsekoun, R. Go, M. Lane, T. Macdonald and C. K. N. Patel, *High power, high efficiency quantum cascade laser systems for directional infrared countermeasures and other defense and security applications*, Proceedings of the SPIE, **7483**, 74830D, (2009).

7. C. Bauer, A. K. Sharma, U. Willer, J. Burgmeier, B. Braunschweig, W. Schade, S. Blaser, L. Hvozdara, A. Müller and G. Holl, *Potentials and limits of mid-infrared laser spectroscopy for the detection of explosives*, Applied Physics B, **92**, 327-333, (2008).

8. J. H. Shorter, D. D. Nelson, J. B. McManus, M. S. Zahniser and D. K. Milton, *Multicomponent Breath Analysis With Infrared Absorption Using Room-Temperature Quantum Cascade Lasers*, IEEE Sensors Journal, **10**, 76-84, (2010).

9. R. F. Kazarinov and R. A. Suris, *Possibility of amplification of electromagnetic waves in a semiconductor with a superlattice*, Soviet Physics: Semiconductors, **5**, 707, (1971).

10. L. C. West and S. J. Eglash, *First observation of an extremely large dipole infrared transition within the conduction band of a GaAs quauntum well*, Applied Physics Letters, **46**, 1156-1158, (1985).

11. M. Helm, P. England, E. Colas, F. Derosa and S. J. Allen, *Intersubband emission from semiconductor superlattices excited by sequential resonant tunneling*, Physical Review Letters, **63**, 74-77, (1989).

12. F. Capasso, K. Mohammed and A. Y. Cho, *Sequential resonant tuneling through a multiquantum well superlattice*, Applied Physics Letters, **48**, 478-480, (1986).

13. P. F. Yuh and K. L. Wang, *Novel infrared band-aligned superlattice laser*, Applied Physics Letters, **51**, 1404-1406, (1987).

14. H. C. Liu, *A novel superlattice infrared source*, Journal of Applied Physics, **63**, 2856-2858, (1988).

15. J. Faist, F. Capasso, D. L. Sivco, C. Sirtori, A. L. Hutchinson and A. Y. Cho, *Quantum Cascade Laser*, Science, **264**, 553-556, (1994).

16. C. Gmachl, F. Capasso, D. L. Sivco and A. Y. Cho, *Recent progress in quantum cascade lasers and applications*, Reports on Progress in Physics, **64**, 1533-1601, (2001).

17. J. Faist, F. Capasso, C. Sirtori, D. L. Sivco, A. L. Hutchinson and A. Y. Cho, *Continuous-wave operation of a vertical transition quantum cascade laser above T=80K*, Applied Physics Letters, **67**, 3057-3059, (1995).

18. J. Faist, F. Capasso, C. Sirtori, D. L. Sivco, A. L. Hutchinson and A. Y. Cho, *Room temperature mid-infrared quantum cascade lasers*, Electronics Letters, **32**, 560-561, (1996).

19. J. Faist, F. Capasso, C. Sirtori, D. L. Sivco, J. N. Baillargeon, A. L. Hutchinson, S. N. G. Chu and A. Y. Cho, *High power mid-infrared (l~5mm) quantum cascade lasers operating above room temperature*, Applied Physics Letters, **68**, 3680-3682, (1996).

20. M. Beck, D. Hofstetter, T. Aellen, J. Faist, U. Oesterle, M. Ilegems, E. Gini and H. Melchior, *Continuous wave operation of a mid-infrared semiconductor laser at room temperature*, Science, **295**, 301-305, (2002).

21. O. Cathabard, R. Teissier, J. Devenson, J. C. Moreno and A. N. Baranov, *Quantum cascade lasers emitting near 2.6mm*, Applied Physics Letters, **96**, 141110, (2010).

22. B. S. Williams, *Terahertz quantum-cascade lasers*, Nature Photonics, **1**, 517-525, (2007).

23. Y. Bai, N. Bandyopadhyay, S. Tsao, E. Selcuk, S. Slivken and M. Razeghi, *Highly temperature insensitive quantum cascade lasers*, Applied Physics Letters, **97**, 251104, (2010).

24. N. Bandyopadhyay, Y. Bai, B. Gokden, A. Myzaferi, S. Tsao, S. Slivken and M. Razeghi, *Watt level performance of quantum cascade lasers in room temperature continuous wave operation at λ~3.76 μm*, Applied Physics Letters, **97**, 131117, (2010).

25. Y. Bai, N. Bandyopadhyay, S. Tsao, S. Slivken and M. Razeghi, *Room temperature quantum cascade lasers with 27% wall plug efficiency*, Applied Physics Letters, **98**, 181102, (2011).

26. A. Hugi, R. Terazzi, Y. Bonetti, A. Wittmann, M. Fischer, M. Beck, J. Faist and E. Gini, *External cavity quantum cascade laser tunable from 7.6 to 11.4mm*, Applied Physics Letters, **95**, 061103, (2009).

27. N. Owschimikow, C. Gmachl, A. Belyanin, V. Kocharovsky, D. L. Sivco, R. Colombelli, F. Capasso and A. Y. Cho, *Resonant second-order nonlinear optical processes in quantum cascade lasers*, Physical Review Letters, **90**, 043902, (2003).

28. C. Gmachl, A. Belyanin, D. L. Sivco, M. L. Peabody, N. Owschimikow, A. M. Sergent, F. Capasso and A. Y. Cho, *Optimized second-harmonic generation in quantum cascade lasers*, IEEE Journal of Quantum Electronics, **39**, 1345-1355, (2003).

29. J. Cockburn, *Mid-infrared quantum cascade lasers*, Mid-Infrared Semiconductor Optoelectronics, 323-355, (Springer, 2006).

30. M. Razeghi, *High-Performance InP-Based Mid-IR Quantum Cascade Lasers*, IEEE Journal of Selected Topics in Quantum Electronics, **15**, 941-951, (2009).

31. L. R. Wilson, J. W. Cockburn, M. J. Steer, D. A. Carder, M. S. Skolnick, M. Hopkinson and G. Hill, *Decreasing the emission wavelength of GaAs-AlGaAs quantum cascade lasers by the incorporation of ultrathin InGaAs layers*, Applied Physics Letters, **78**, 413-415, (2001).

32. C. Sirtori, J. Faist, F. Capasso, D. L. Sivco, A. L. Hutchinson, S. N. G. Chu and A. Y. Cho, *Continuous wave operation of midinfrared (7.4-8.6mm) quantum cascade lasers up to 110 K temperature*, Applied Physics Letters, **68**, 1745-1747, (1996).

33. D. Hofstetter, M. Beck, T. Aellen and J. Faist, *High-temperature operation of distributed feedback quantum-cascade lasers at 5.3μm*, Applied Physics Letters, **78**, 396-398, (2001).

34. J. Faist, M. Beck, T. Aellen and E. Gini, *Quantum-cascade lasers based on a bound-to-continuum transition*, Applied Physics Letters, **78**, 147-149, (2001).

35. Y. Yao, X. J. Wang, J. Y. Fan and C. F. Gmachl, *High performance "continuum-to-continuum" quantum cascade lasers with a broad gain bandwidth of over 400 cm^{-1}*, Applied Physics Letters, **97**, 081115, (2010).

36. D. G. Revin, L. R. Wilson, E. A. Zibik, R. P. Green, J. W. Cockburn, M. J. Steer, R. J. Airey and M. Hopkinson, *InGaAs/AlAsSb quantum cascade lasers*, Applied Physics Letters, **85**, 3992-3994, (2004).

37. K. Ohtani and H. Ohno, *An InAs-based intersubband quantum cascade laser*, Japanese Journal of Applied Physics Part 2-Letters, **41**, L1279-L1280, (2002).

38. M. P. Semtsiv, M. Ziegler, S. Dressler, W. T. Masselink, N. Georgiev, T. Dekorsy and M. Helm, *Above room temperature operation of short wavelength (l=3.8mm) strain-compensated $In_{0.73}Ga_{0.27}As$-AlAs quantum-cascade lasers*, Applied Physics Letters, **85**, 1478-1480, (2004).

39. C. Sirtori, P. Kruck, S. Barbieri, P. Collot, J. Nagle, M. Beck, J. Faist and U. Oesterle, *GaAs/$Al_xGa_{1-x}As$ quantum cascade lasers*, Applied Physics Letters, **73**, 3486-3488, (1998).

40. H. Page, C. Becker, A. Robertson, G. Glastre, V. Ortiz and C. Sirtori, *300 K operation of a GaAs-based quantum-cascade laser at l ~ 9mm*, Applied Physics Letters, **78**, 3529-3531, (2001).

41. H. Page, S. Dhillon, M. Calligaro, C. Becker, V. Ortiz and C. Sirtori, *Improved CW operation of GaAs-Based QC lasers: T-max=150 K*, IEEE Journal of Quantum Electronics, **40**, 665-672, (2004).

42. J. Faist, F. Capasso, C. Sirtori, D. L. Sivco and A. Y. Cho, *Quantum Cascade Lasers*, Intersubband Transitions in Quantum Wells: Physics and Device Applications II, (Academic Press, 1999).